THE JOURNAL OF BIOLOGICAL CHEMISTRY VOL. 288, NO. 14, pp. 9867–9880, April 5, 2013

Insulin Signaling in Type 2 Diabetes

EXPERIMENTAL AND MODELING ANALYSES REVEAL MECHANISMS OF INSULIN RESISTANCE IN HUMAN ADIPOCYTES[*][S]

Received for publication, October 30, 2012, and in revised form, February 1, 2013 Published, JBC Papers in Press, February 11, 2013, DOI 10.1074/jbc.M112.432062

Cecilia Brännmark[‡1], **Elin Nyman**[‡1], **Siri Fagerholm**[‡], **Linnéa Bergenholm**[‡], **Eva-Maria Ekstrand**[‡], **Gunnar Cedersund**[‡§], **and Peter Strålfors**[‡2]

From the Departments of [‡]*Clinical and Experimental Medicine and* [§]*Biomedical Engineering, Linköping University, SE58185 Linköping, Sweden*

Background: Mechanisms of insulin resistance in type 2 diabetes are not known.
Results: A first dynamic mathematical model based on data from human adipocytes yields systems level understanding of insulin resistance.
Conclusion: Attenuation of an mTORC1-derived feedback in diabetes explains reduced sensitivity and signal strength throughout the insulin-signaling network.
Significance: Findings give a molecular basis for insulin resistance in the signaling network.

Type 2 diabetes originates in an expanding adipose tissue that for unknown reasons becomes insulin resistant. Insulin resistance reflects impairments in insulin signaling, but mechanisms involved are unclear because current research is fragmented. We report a systems level mechanistic understanding of insulin resistance, using systems wide and internally consistent data from human adipocytes. Based on quantitative steady-state and dynamic time course data on signaling intermediaries, normally and in diabetes, we developed a dynamic mathematical model of insulin signaling. The model structure and parameters are identical in the normal and diabetic states of the model, except for three parameters that change in diabetes: (i) reduced concentration of insulin receptor, (ii) reduced concentration of insulin-regulated glucose transporter GLUT4, and (iii) changed feedback from mammalian target of rapamycin in complex with raptor (mTORC1). Modeling reveals that at the core of insulin resistance in human adipocytes is attenuation of a positive feedback from mTORC1 to the insulin receptor substrate-1, which explains reduced sensitivity and signal strength throughout the signaling network. Model simulations with inhibition of mTORC1 are comparable with experimental data on inhibition of mTORC1 using rapamycin in human adipocytes. We demonstrate the potential of the model for identification of drug targets, *e.g.* increasing the feedback restores insulin signaling, both at the cellular level and, using a multilevel model, at the whole body level. Our findings suggest that insulin resistance in an expanded adipose tissue results from cell growth restriction to prevent cell necrosis.

Insulin is a prime controller of energy homeostasis in the human body. Dysfunction in the insulin control perturbs energy homeostasis with consequences in the form of disease such as type 2 diabetes (T2D)[3] and its corollaries cardiovascular disease, nephropathy, and neuropathy. Insulin control of target cells is relayed from the insulin receptor (IR) at the cell surface to different cellular processes, such as glucose uptake and protein synthesis, through an intracellular signaling network. In obesity the expanding adipose tissue, for poorly understood reasons, responds to the hypertrophy and hyperplasia of the adipocytes with a resistance to the hormone. Energy homeostasis is tolerably maintained despite insulin resistance in the adipose, muscle, and liver tissues as the insulin producing β-cells compensate by releasing more insulin. Eventually, after many years, the β-cells often fail to compensate and T2D can be diagnosed. Present understanding of insulin signaling is based on identification and sequencing of individual signaling intermediaries in a wide variety of different cell types and model organisms. There are many observations of differences between signaling in diabetic and normal target tissues of insulin, but there is neither consensus on their relative importance nor on how they relate to each other. We need a systems approach to examine and understand insulin resistance, where systems wide quantitative data are obtained in a consistent fashion and analyzed using mathematical modeling. Earlier models of insulin signaling are based on limited data and data from different cell types, and parameter values are often arbitrarily chosen (1). Important examples of experimental and modeling analyses that have provided mechanistic insights into insulin signaling are insulin binding to its receptor (2), the early phase of insulin signaling in human adipocytes (3), and insulin control of mTORC2 activity in the HeLa cell line (4).

In an integrated experimental/modeling approach we have earlier analyzed the very early phase of insulin signaling in human adipocytes, restricted to signaling between the insulin receptor (IR) and the immediate downstream insulin receptor

* This work was supported by the Swedish Diabetes Fund, Novo Nordic Foundation, University of Linköping, and the Swedish Research Council.
[S] This article contains supplemental Figs. S1–S3, Tables S1 and S2, and Models S1–S4.
[1] Both authors contributed equally to this work.
[2] To whom correspondence should be addressed. Tel.: 46-10-1034315; Fax: 46-10-1034149; E-mail: peter.stralfors@liu.se.

[3] The abbreviations used are: T2D, type 2 diabetes; IR, insulin receptor; mTOR, mammalian target of rapamycin; mTORC1, mTOR in complex with raptor; mTORC2, mTOR in complex with rictor; PKB, protein kinase B/Akt; S6K1, p70S6 protein kinase; GLUT4, insulin-regulated glucose transporter.

substrate-1 (IRS1) (3). The model required both internalization of the receptor and a feedback from IRS1 to IR to explain experimental data. However, no analysis is available for the insulin-signaling network in adipocytes, normally and in T2D, as reviewed in Ref. 1.

We now report a quantitative and comprehensive systems analysis of insulin signaling dynamics normally and in T2D. This systems analysis rests on two pillars: (i) collection of dynamic and steady-state data of key signaling intermediaries in primary human mature adipocytes from non-diabetic individuals and, in parallel, from obese patients with T2D; and (ii) mathematical modeling analysis that translates the systems wide data to systems wide mechanistic insights. Our analyses indicate that almost all signaling intermediaries are altered in T2D, and that most alterations may be explained by a single original effect: attenuation of a positive feedback from mammalian target of rapamycin (mTOR) in complex with raptor (mTORC1) to IRS1.

EXPERIMENTAL PROCEDURES

Subjects—Informed consent was obtained from all participants. Procedures have been approved by the ethics board, Linköping University, and were performed in accordance with the Declaration of Helsinki. Subcutaneous fat was obtained from elective abdominal surgery during general anesthesia. A slice of subcutaneous tissue from skin to muscle fascia was excised. Subjects were recruited consecutively from elective surgery at the University Hospital in Linköping-Norrköping. To ensure inclusion only of patients with T2D related to obesity, they were selected when diagnosed with T2D and as obese or overweight (BMI $>$ 27). In the comparison group, the only selection criterion for non-diabetic subjects was that they were not diagnosed with diabetes (supplemental Table S1). Thus, there will be some obese insulin-resistant subjects in the non-diabetic comparison group. This approach allows for examination of the common obesity-related type 2 diabetes and for a wide significance of the results. We have earlier found that there is no difference in the response to insulin between adipocytes from male and female patients with T2D (5).

Materials—Rabbit anti-phospho-p70S6K-Thr-389 (number 9205), anti-phospho-S6-Ser-235/236 (number 2211), anti-phospho-PKB-Ser-473 (number 9271), and anti-phospho-IRS1-Ser-302 (number 2384, murine sequence) were from Cell Signaling Technology (Danvers, MA). Mouse anti-phosphotyrosine (PY20) monoclonal antibodies were from Transduction Laboratories (Lexington, KY) Rabbit anti-phospho-PKB-Thr-308 antibodies were from Upstate Biotech (Charlottesville, VA) and Invitrogen (number 44-602G). Rabbit anti-phospho-AS160-Thr-642 antibodies were from Millipore (number 07-802; Darmstadt, Germany). Monoclonal mouse anti-β-tubulin antibodies were from Sigma (T5201) and anti-actin antibodies were from Santa Cruz (sc-1616, Santa Cruz, CA).

Isolation and Incubation of Adipocytes—Adipocytes were isolated from subcutaneous adipose tissue by collagenase (type 1, Worthington) digestion as described (6). Cells were treated and incubated, at a concentration of 100 μl of packed cells per ml, in a shaking water bath in supplemented Krebs-Ringer solution as described (5).

SDS-PAGE and Immunoblotting—Cell incubations were terminated by separating cells from medium using centrifugation through dinonyl phtalate. To minimize postincubation signaling and protein modifications cells were immediately dissolved in SDS and β-mercaptoethanol with protease and protein phosphatase inhibitors, frozen within 10 s, and thawed in boiling water for further processing, as described (6). Immunoblotting after SDS-PAGE (5) was evaluated by chemiluminescence imaging (Las 1000, Image-Gauge, Fuji, Tokyo, Japan). The linearity of the chemiluminescence signal to the amount of each specific protein was ascertained after adjusting the concentration of primary and secondary antibodies used in the immunoblottings. β-Tubulin or actin was used as a loading control and all samples were normalized for the amount of β-tubulin or actin. For comparison of the level of phosphorylation between non-diabetic and diabetic subjects a standard mixture of adipocyte proteins was run in duplicate on each gel in order that all samples were normalized to the mean intensity of the corresponding phosphorylated protein in the standard mixture.

Glucose Uptake—After transfer of cells to medium without glucose cells were incubated with the indicated concentration of insulin for 15 min, and then 2-deoxy-D-[1-^{3}H]glucose (10 μCi/ml) was added at a final concentration of 50 μM. Glucose transport was then determined as uptake of 2-deoxy-D-[1-^{3}H]glucose during 30 min (7). As uptake in human primary mature adipocytes is linear for at least 30 min (5), the rate of uptake is constant and accumulated uptake of glucose is a measure of the rate of glucose uptake.

Presentation of Experimental Data—All experimental values are mean ± S.E. for the indicated number (n) of cell preparations, which is the same as number of different subjects.

Mathematical Models—We used ordinary differential equations to create the mechanistic model of insulin signaling (Fig. 1 and supplemental Fig. S1). For model simplicity we primarily used mass-action kinetics and, only when required to explain the data, Hill/Michaelis-Menten kinetics. A simple example of an ordinary differential equation underlying Fig. 1*B* is shown in Equation 1,

$$\frac{d(IRins)}{dt} = k1a \times insulin \times IRm - k1c \times IRins \qquad \text{(Eq. 1)}$$

where k_{1a} and k_{1c} are rate constants. All model equations are given in the supplemental text, Section 2. Before simulating stimulation of cells by insulin, a steady-state simulation was performed to ensure steady-state initial conditions at basal conditions according to experimental data. We did not change the model parameters between steady-state and the stimulated state. Absolute concentrations are not known and therefore the total amount of each protein was set to 100%, except as indicated in the diabetic state of the model.

The values of the model parameters are not possible to determine experimentally for the system we study. We thus used an optimization algorithm to test different values of the parameters within realistic limits, and then evaluated the agreement between the simulated output of the model and the experimental data. The optimization is centered around a cost function,

$V(p)$, that for the quantitative agreement with experimental data is given by the sum of least squares,

$$V(p) = \sum_{i=1}^{N} \frac{(y(i) - \hat{y}(i,p))^2}{SE(i)^2} \qquad \text{(Eq. 2)}$$

where $y(i)$ contains the experimental data points, $\hat{y}(i,p)$ the simulated output of the model for the parameter vector p, and SE(i) is the mean ± S.E. of the experimental data. The index i of the summation of least squares includes all measured proteins for all measured time points. For the optimization we used the Systems Biology Toolbox for Matlab (8) and its simannealingSBAO function, which is a combination of a global simulated annealing approach with a local, but not gradient-based, downhill simplex approach. The models and a complete description of the modeling are available in the supplemental material.

RESULTS

Insulin Signaling Normally—We investigated the signaling of insulin to control of glucose transport and protein synthesis (Fig. 1*A*) in primary human mature adipocytes. We determined glucose uptake and the state of phosphorylation of intermediary signal transducing proteins in response to insulin at (i) quasi steady-state conditions using different concentrations of insulin to determine the sensitivity to insulin,[4] and (ii) the dynamics of insulin signaling by determining the extent of phosphorylation at different time points in response to maximal insulin stimulation (Fig. 2, *blue symbols*).

A visual inspection of the data identifies some features of the signaling pathways. First, there is a marked increase in insulin sensitivity (decreased EC_{50}) at two steps: (i) from IR autophosphorylation to phosphorylation of IRS1 by IR, and (ii) from phosphorylation of protein kinase B (PKB/Akt) at Thr-308 to phosphorylation of AS160 (Fig. 2, summarized in Fig. 3, *A* and *C*). At the steps from phosphorylation of IRS1 to phosphorylation of PKB at Thr-308, and from phosphorylation of AS160 to enhanced glucose uptake, on the other hand, there are no changes in sensitivity to insulin (Fig. 2, summarized in Fig. 3, *A* and *C*). Second, the response time to insulin, to reach half steady-state effect ($t_{½}$) remains short throughout the pathway to glucose uptake, and quasi steady-states are established after <5 min and last for at least 60 min (Fig. 2, summarized in Table 1). Furthermore, IR and IRS1 phosphorylation exhibit overshoot behavior that peaks at around 1.5 min, before it reaches steady-state (Fig. 2).

In addition to the signaling pathway leading to control of glucose uptake, we determined signaling through the components of the signaling branch mTORC1-S6K1-S6 that mediates insulin control of protein synthesis (Fig. 1*A*). Activation of mTORC1 by insulin is complex and as a minimum involves PKB and ERK1/2 phosphorylation of TSC2, as well as PKB-catalyzed phosphorylation and mTORC1-catalyzed autophosphorylation of the mTORC1 component PRAS40 (reviewed in Ref. 9). We therefore followed the activation of mTORC1 as phosphorylation of p70S6 protein kinase-1 (S6K1) and its substrate the ribosomal protein S6 (S6), which serve as sequential readouts of mTORC1 activity (Fig. 2). We have in human adipocytes earlier identified a rapamycin-sensitive, positive feedback signal from insulin activation of mTORC1 to phosphorylation of IRS1 at Ser-307 (corresponding to Ser-302 in the murine sequence) (10–13). This feedback appears to enhance phosphorylation of IRS1 at tyrosine in response to insulin (10–15). Although existence of the feedback signal is undisputed, its importance in human adipocytes and whether it represents a positive or negative feedback has remained unsettled (reviewed in Ref. 16).

Insulin Signaling in T2D—We also examined the response of the different signaling intermediaries to insulin in adipocytes obtained from patients diagnosed with T2D (Fig. 2, *red symbols*). Considering the same basic features as above for the insulin signaling pathway to control glucose transport normally, the diabetic state displays a reduced sensitivity to insulin (up to 10 times higher EC_{50} than in non-diabetic state) for all states except for autophosphorylation of IR, and phosphorylation of PKB at Thr-308 where the effect is small (Fig. 2, summarized in Fig. 3). Conversely, the data do not reveal any significant differences in the response time to insulin for any of the intermediaries. However, phosphorylation of S6K1 and S6 display a much slower response to insulin, both normally and in T2D, than the likewise mTORC1 downstream phosphorylation of IRS1 at Ser-307 (Fig. 2, Table 1). A further important feature of the diabetic state concerns the steady-state level of phosphorylation of the different signaling intermediaries in response to maximal insulin concentrations. Except for phosphorylation of PKB at Ser-473, there is a marked and consistent reduction of the steady-state phosphorylation of all signaling intermediaries in the diabetic compared with normal cells (Fig. 2, Table 1).

A key feature of insulin resistance in the diabetic state is that activation of mTORC1 by insulin is attenuated in adipocytes from diabetic subjects. This attenuation of mTORC1 activation in T2D is demonstrated by (i) attenuation of mTORC1-mediated phosphorylation of IRS1 at Ser-307 (Fig. 2, *c2* and *d2*), and of S6K1 (Fig. 2, *d4*) and its substrate S6 (Fig. 2, *d5*), (ii) by the loss of mTORC1 inhibition of autophagy (13), and (iii) impaired maintenance of mitochondrial function (13).

Qualitative Modeling Shows the Need for a New Feedback to IRS1—We analyzed the experimental data using modeling in two stages: first using minimal modeling based on specific qualitative observations, and then, in a second stage, by the construction of a detailed dynamic model based on all the data. The minimal modeling approach is a valuable and independent analysis, which we undertook for several reasons. First, large scale data sets, as shown in Fig. 2, result in big models with a corresponding high-dimensional parameter space that is more or less impossible to search in an exhaustive manner. Therefore model predictions will not be unique conclusions based solely on the data and the chosen model structure (so-called core predictions (3, 17)), but also depend on the arbitrarily chosen parameter values. Minimal models with few parameters, on the

[4] Insulin sensitivity/resistance sometimes refers to the magnitude of the maximal insulin response. Herein we have restricted it to refer to the concentration of insulin that produces a half-maximal response, such that higher insulin sensitivity and lower insulin resistance results in a left-shift in the dose-response curve to lower concentrations of insulin and lower EC_{50} values. Lower insulin sensitivity and higher insulin resistance consequently refer to a right-shift to higher EC_{50} values.

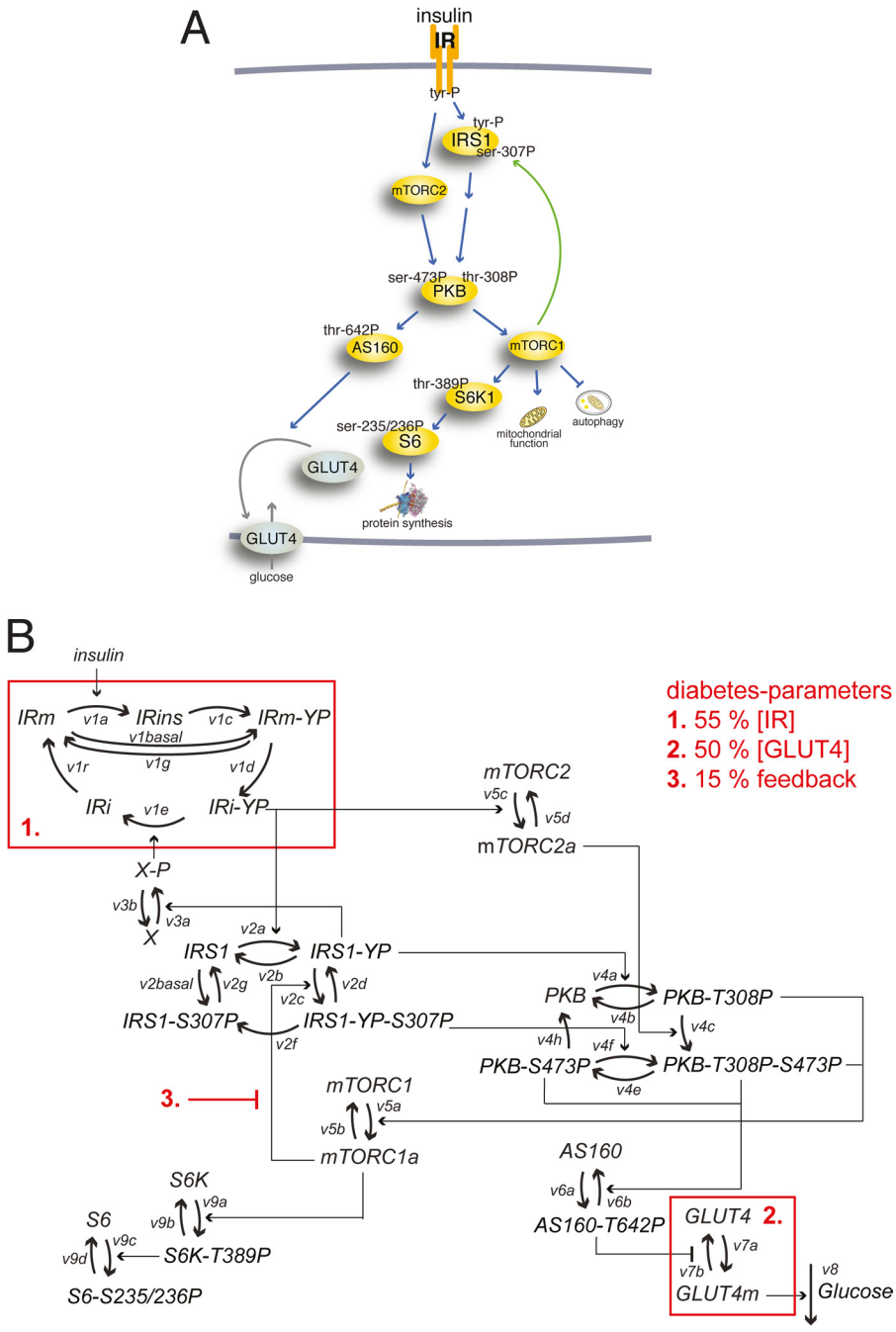

FIGURE 1. **Insulin signaling network.** Examined phosphorylation sites in signaling intermediaries are indicated (-P). *A*, schematic of insulin signaling pathways examined. *Blue arrows* indicate signaling pathways; *green arrow* indicates positive feedback signal; *gray arrow* indicates GLUT4 translocation to the plasma membrane in response to insulin signaling. *B*, structure of the mechanistic mathematical model of the insulin-signaling network. Model equations are detailed in supplemental text, Section 2–3. Rate constants (at reaction arrows) and measured phosphorylation sites are indicated. The three diabetes parameters introduced in the diabetes state of the model are indicated in *red*. *a*, active state; *m*, plasma membrane-localized state; *i*, internalized state. *AS160*, Akt substrate of 160 kDa.

other hand, have the advantage that they can be analyzed with unique predictions. Second, hypothesis testing with minimal models is an approach centered on rejections, which are strong conclusions that constitute valuable insights drawn from data. We have already developed a minimal model for the IR-IRS1 subsystem (*Mif*a in Ref. 3), which involves insulin-controlled phosphorylation of IR and IRS1 and only a feedback from an unknown downstream intermediate X to dephosphorylation of IR. The state X describes an unspecified feedback from IRS1 to IR. Additionally, for the IR-IRS1 subsystem we can identify key qualitative experimental observations that are well determined and that involve the appearance of insulin resistance: IR exhibits a clearly reduced steady-state phosphorylation in T2D (Fig. 4*A*) but the sensitivity to insulin is not affected (Fig. 2, *a1*). IRS1, on the other hand, exhibits both reduced steady-state phosphorylation (Fig. 2, *b2*) and reduced sensitivity to insulin (Fig. 4*A*). For these reasons we undertook a minimal modeling approach to identify mechanistic differences

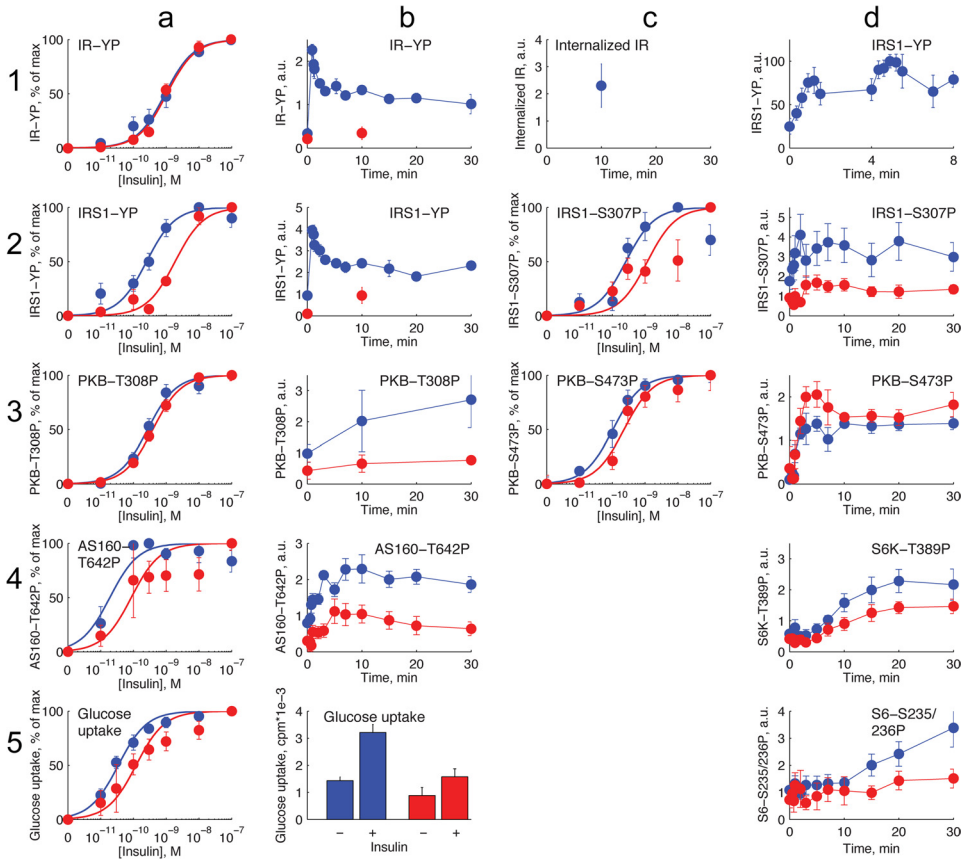

FIGURE 2. **Experimental analysis of insulin signaling normally and in T2D.** Freshly isolated mature human adipocytes from non-diabetic (*blue*) or T2D subjects (*red*) were incubated with insulin as indicated, and the extent of protein phosphorylation or glucose uptake was determined. *a1-a4* show dose-responses and *b1-b4* show the corresponding time courses for the indicated insulin signaling intermediaries. *a5*, rate of glucose uptake with indicated concentration of insulin. *b5*, rate of glucose uptake with or without insulin (10 nM), as indicated. *c1*, amount of internalized IR (% of total IR) at the indicated time after addition of 100 nM insulin. Data from (3). *d1*, time course for phosphorylation of IRS1 at tyrosine, with 1.2 nM insulin added at $t = 0$, and additional insulin to 10 nM added at $t = 4$ min. Data are from Ref. 3. *c2-c3* and *d2-d5*, dose-responses and time courses for insulin signaling intermediaries as indicated. *a1-a4* and *c2-c3*, cells incubated with the indicated concentration of insulin for 10 min. *b1-b2*, cells incubated with 10 nM insulin for the indicated time. Data on normal cells were from Ref. 3. *b3-b4* and *d2-d5*, cells incubated with 10 nM insulin for the indicated time. Details about patients, and number of patients, donating adipocytes in the different experiments are detailed in supplemental Table S1. Time course experiments show the extent of protein phosphorylation expressed in arbitrary units (*a.u.*) that in each experiment are the same for non-diabetic and diabetic conditions and thus directly comparable. To compare dose-response/insulin sensitivity/EC_{50}, the extent of protein phosphorylation or rate of glucose uptake is normalized to between 0 and 100% phosphorylation or glucose uptake rate, respectively. Time courses were determined for 60 min, but for clarity only the first 30 min are shown. *Blue* (non-diabetic) and *red* (diabetic) *dots* denote experimental data ± S.E. *Lines* denote fitting dose-response curves to sigmoidal curves (GraphPad Prism) or for time courses connection of data points.

between normal and T2D signaling that can or cannot explain these qualitative observations.

We first analyzed the ability of a reduction in amount of IR (as it is reduced to 55% of normal in T2D adipocytes (12, 18)) to explain the qualitative observations regarding IR and IRS1 phosphorylation. More specifically, we used all parameters determined for the *Mif*a model (3) that can simulate the normal state in an acceptable manner and simulated a reduced amount of IR (Fig. 4*B, 1*). As can be seen, reduction in the amount of IR can explain the difference in the steady-state level of phosphorylation, but not the altered sensitivity to insulin for phosphorylation of IRS1. Also a corresponding reduction of IRS1 fails to explain the reduced sensitivity to insulin, and the reduced steady-state phosphorylation of IR (Fig. 4*B, 2*). We further examined the *Mif*a model by altering the feedback from X to IR, which also was unable to produce a decreased sensitivity to insulin (Fig. 4*B, 3*). None of these three mechanistic hypotheses is an acceptable explanation for the observed reduction in insulin sensitivity and are hence rejected. Finally, we examined a fourth hypothesis, involving a feedback to IRS1, which can explain the reduced sensitivity to insulin for phosphorylation of IRS1 (Fig. 4*C*). Such feedbacks have been proposed in the literature (10–16, 19, 20) and the analysis above demonstrates that either alteration of such a negative/positive feedback or some other not yet tested mechanism is necessary to explain the reduced insulin sensitivity in human adipocytes.

A Detailed Dynamic Model of Insulin Signaling Normally and in T2D—In the next modeling stage we constructed a detailed dynamic model of the insulin-signaling network. We first included all known reactions between the measured signaling intermediaries and other signaling intermediaries that was important for the structure of the signaling network and fitted the model to the data in Fig. 2. Next, to reduce the number of parameters in the model we removed redundant reactions, *i.e.* reactions not needed to explain the data (supplemental Fig. S1). The final model (Fig. 1*B*) can reasonably well explain the experimental data (Fig. 5, *blue*).

In adipocytes from patients with T2D, the concentration of IR is reduced to 55% compared with non-diabetic adipocytes (12, 18) and this reduction was therefore used to model the

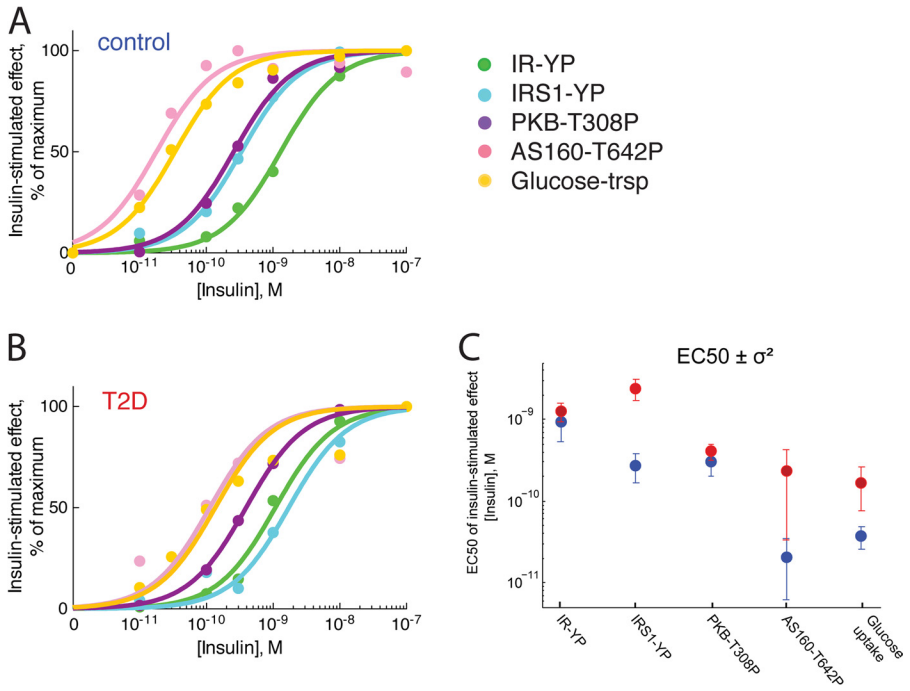

FIGURE 3. **Comparison of sensitivity to insulin at the different signaling steps, normally and in adipocytes from subjects with T2D.** Dose-response effects of the indicated concentrations of insulin on the indicated signaling intermediaries and glucose transport using data from Fig. 2. *A,* adipocytes from non-diabetic subjects display a shift in insulin sensitivity from IR to IRS1/PKB and from IRS1/PKB to AS160/glucose uptake. *B*, adipocytes from subjects with T2D display a reduced sensitivity to insulin, most marked for IRS1 and AS160/glucose uptake, but the increased insulin sensitivity from IRS1 to AS160/glucose uptake remains in subjects with T2D. The insulin sensitivity at IR and at PKB is not altered in subjects with T2D. *C,* a profile likelihood analysis (48) estimation of mean and variance for the EC_{50} variables of non-diabetic (*blue circles*) and diabetic (*red circles*) subjects shows that EC_{50} of IRS1-YP and glucose uptake are separated between non-diabetic and diabetic subjects, whereas EC_{50} of IR-YP and PKB-T308P are clearly overlapping and EC_{50} of AS160-T642P slightly overlapping. Also, EC_{50} of IRS1-YP for non-diabetics is lower and separated from EC_{50} of IR-YP, whereas for diabetics IRS1-YP is higher and also separated. We performed the profile likelihood analysis using a Hill equation to allow for variable slope and maximum values of the parameters of a sigmoid dose-response curve.

TABLE 1

Summary of insulin responses for phosphorylation of different signaling intermediaries and for glucose uptake

Steady-state levels of phosphorylation and glucose uptake, determined at maximal insulin concentrations, are presented as fold-increase over non-diabetic controls at basal (without insulin) conditions.

	Sensitivity EC_{50}		Response time		Basal level		Steady-state level	
	Normal[a]	T2D	Normal	T2D	Normal	T2D	Normal	T2D
	nM insulin		*t 1/2 min*		*Fold-over basal control*		*Fold-over basal control*	
IR-YP	0.95	1.2	1.0	ND[b]	1	0.8	4.3	1.5
IRS1-YP	0.28	2.4	1.0	ND	1	0.2	2.6	1.0
IRS1-S307P	0.23	0.85	0.7	2.0	1	0.6	4.4	1.9
PKB-T308P	0.30	0.41	ND	ND	1	0.7	5.0	5.0
PKB-S473P	0.10	0.38	1.0	1.0	1	1.0	5.0	5.0
AS160-T642P	0.021	0.23	1.5	2.0	1	0.4	2.9	1.3
Glucose uptake	0.037	0.17	ND	ND	1	0.3	2.1	1.0
S6K1-T389P	ND	ND	7.5	7.5	1	0.7	4.1	2.6
S6-S235P/S236P	0.3	ND	15		1	1.5	4.3	2.5

[a] Normal, non-diabetic controls.
[b] ND, not determined.

diabetic state. The intracellular level of IRS1, on the other hand, is in human adipocytes not affected by insulin resistance or T2D (10, 12), although the contrary has been suggested (21). The concentration of the insulin-regulated glucose transporter (GLUT4) is also reduced (to 30–70%) in adipocytes from diabetic patients compared with cells from non-diabetics (22–24). In our model we therefore introduced the lower concentrations of IR and GLUT4, and a parameter that can increase or decrease the mTORC1-mediated phosphorylation of IRS1 at Ser-307 (*v2c* in Fig. 1*B*) to simulate the insulin resistant/diabetic state (Fig. 5, *red lines*). Except for these three diabetes parameters, all other parameters were optimized to fit both the diabetic and non-diabetic states of the model (supplemental Table S2). Best fit to diabetes data were obtained with 50% of the normal concentration of GLUT4 and a positive feedback from mTORC1 to IRS1 reduced to 15% of normal.

Examination of the Contribution of the Individual Diabetes Parameters to the Diabetic State—As the final model includes three specific differences (diabetes-parameters) between insulin signaling normally and in T2D, we examined their relative influence on the diabetic state. The reduced concentration of IR alone only marginally influences signaling (mainly the reduced steady-state autophosphorylation of IR) (Fig. 6*A* and supplemental Fig. S2*A*). The reduced concentration of GLUT4 only affects glucose uptake and explains the diabetic effect on maximal insulin-stimulated glucose uptake (Fig. 6*B*

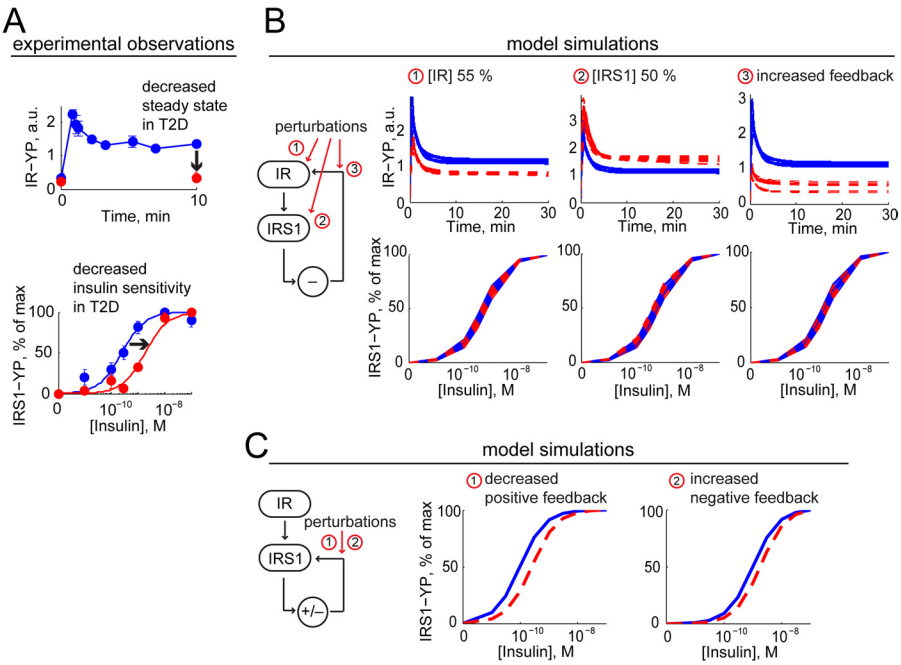

FIGURE 4. **Qualitative model analysis of the initial phase of insulin signaling.** *A*, experimental observations of steady-state phosphorylation of IR (10 nM insulin for the indicated time) and insulin sensitivity for phosphorylation of IRS1 at tyrosine (indicated concentration of insulin for 10 min), normally (*blue*) and in T2D (*red*). *B*, model simulations of time course for phosphorylation of IR, or dose-response curves for phosphorylation of IRS1 at tyrosine in response to increasing concentrations of insulin, with reduced levels of IR or IRS1, or increased feedback to IR. The effects of the indicated perturbations were examined through core prediction analysis (3) using a model for the initial phase of insulin signaling (3). *C*, model simulations of dose-response curves for phosphorylation of IRS1 at tyrosine in response to increasing concentrations of insulin, with decreased positive or increased negative feedback to IRS1. The effects of the indicated perturbations were examined through qualitative analysis of the minimal model in the figure (supplemental text, Section 1).

and supplemental Fig. S2*B*), but is irrelevant for the reduced sensitivity to insulin. Instead, the reduced sensitivity to insulin, for glucose uptake and for all signaling intermediaries, is explained by attenuation of the positive feedback from mTORC1 to IRS1. This attenuated positive feedback also explains most of the reduction of the maximally insulin-stimulated steady-state levels of phosphorylated signaling intermediaries in the diabetic cells (Fig. 6*C* and supplemental Fig. S2*C*). It should be noted that we did not explicitly model the feedback from mTORC1 to IRS1 as positive or negative. Instead we allowed for both variants in the optimization, and reached the best agreement between model simulation and the quantitative data when we used attenuation of a positive feedback to explain the diabetic state.

Attenuation of mTORC1 activation and feedback from mTORC1 to IRS1 is hence the most important change going from normal to diabetic signaling, as this change alone impacts the whole insulin signaling network. This is further emphasized considering that transcription of the *GLUT4* gene is regulated by mTORC1 through control of the transcription factor sterol regulatory element-binding protein 1 (25–27). Therefore, attenuation of mTORC1 may impair both long-term transcription of *GLUT4* and acute signaling to translocation. The reduced concentration of IR may be a result of the hyperinsulinemia associated with insulin resistance (18). Interestingly, attenuated mTORC1 signaling enhances autophagy in diabetic human adipocytes (13) and may thus also explain the reduced concentration of IR (28).

Model Analysis and Validation—Our integrated experimental modeling approach to a systems analysis of normal and diabetic insulin signaling in human adipocytes identifies attenuated activation of mTORC1 and the corresponding attenuation of the feedback to IRS1 as a key mechanism in insulin resistance of T2D. Rapamycin in complex with the cellular protein FKBP12 is a specific inhibitor of mTORC1. We analyzed in some detail how inhibition of mTORC1 affects insulin signaling through the insulin signaling network in our dynamic model, thus *in silico* mimicking the effect of rapamycin (supplemental Fig. S3). In a dose-dependent manner rapamycin simulation (50–93% inhibition of mTORC1 signaling) reduced the effect of insulin on all phosphorylated intermediaries. Unexpectedly, also IR autophosphorylation was decreased by rapamycin, which is due to that IRS1 exists in several activated states in the model. It is only the tyrosine- (but not Ser-307) phosphorylated IRS1 state that activates the negative X-feedback to IR (Fig. 1*B*), and this particular IRS1 state is increased in response to rapamycin (supplemental Fig. S3*B*). However, the sum of the two tyrosine-phosphorylated states of IRS1 (Table 2 and supplemental Fig. S3) is reduced in the rapamycin simulation as expected.

The effects of simulating rapamycin inhibition of mTORC1 in the model are corroborated by experimental inhibition of mTORC1 in human mature adipocytes with rapamycin. (i) Rapamycin markedly inhibited the insulin-stimulated increase in the phosphorylation of S6 (Fig. 7*A*). (ii) Rapamycin has been reported to inhibit the insulin-stimulated increase in autophosphorylation of IR (Fig. 7*B*) (29). (iii) The marked right-shift of the dose-response curve for insulin stimulation of IRS1 phosphorylation at tyrosine, to higher concentrations of insulin, has been experimentally verified (Fig. 7*C*) (10). (iv) The reduction

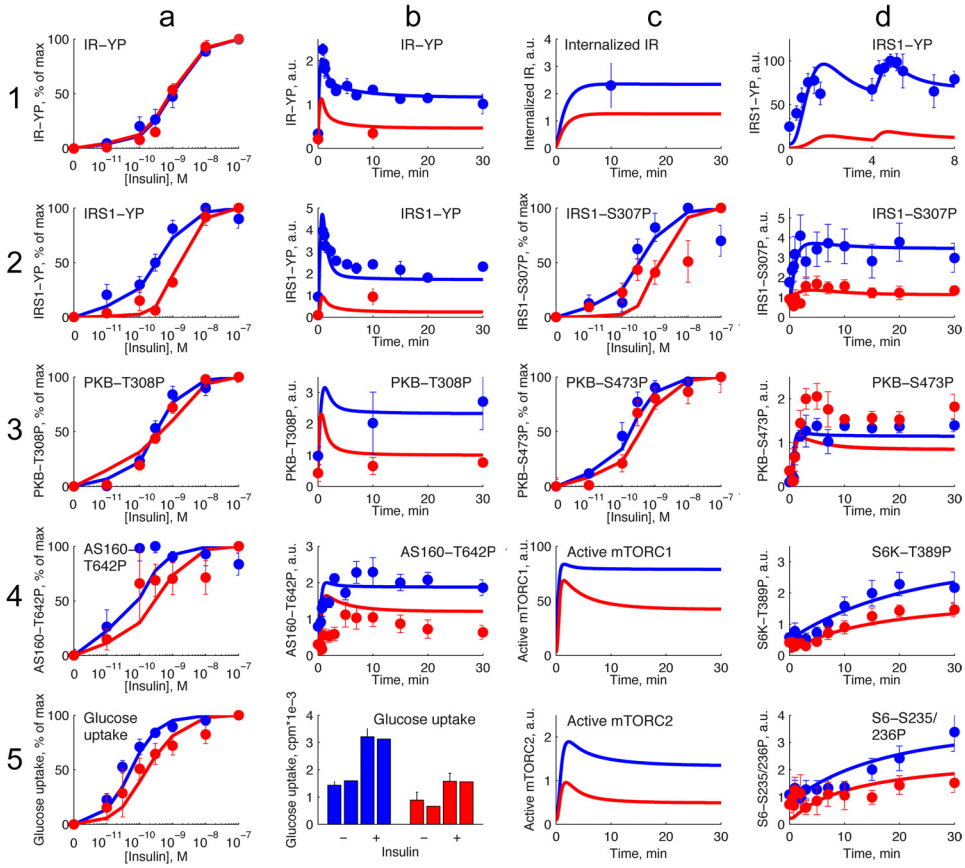

FIGURE 5. **Detailed dynamic model of insulin signaling normally and in T2D.** Comparison of model simulation (*lines*) and experimental data (*dots*) for insulin signaling, normally (*blue*) and in T2D (*red*). Model simulations were performed to mimic the experimental conditions, and the same simulations were performed for the normal and the T2D state. *a1-a4* and *c2-c3*, dose-response was simulated using increasing values of the insulin input (0–100 nM as indicated) and the response after 10 min was plotted. The simulated values were normalized between 0 and 100%. *a5*, dose-response of glucose uptake was simulated using increasing values of the insulin input (0–100 nM as indicated) during 15 min followed by 30 min with a glucose (0.05 mM) input, without removing the insulin input. The simulated values were normalized between 0 and 100%. *b5*, absolute glucose uptake was simulated using 0 and 100 nM insulin as input for 15 min followed by 30 min with a glucose (0.05 mM) input, without removing the insulin input. We used a normalization constant to fit the normal glucose uptake to data, and the same constant for the T2D glucose uptake. *b1-b4*, *c4-c5*, and *d2-d5*, time course was simulated using 10 nM insulin during 30 min. We used a normalization constant to fit the normal time courses to data, and the same constant for the T2D time course. *c1*, time course was simulated using 10 nM insulin during 30 min. *d1*, double-step stimulation was simulated using 1.2 nM insulin as input for 4 min followed by 10 nM insulin for 4 min. We used a normalization constant to fit the normal time course to data, and the same constant for the T2D time course. Experimental details are described as in the legend to Fig. 2.

of the steady-state phosphorylation of IRS1 at Ser-307 has been shown experimentally (Fig. 7*D*) (10). (v) A small reduction of the steady-state phosphorylation of AS160 has been experimentally demonstrated (Fig. 7*E*) (29). (vi) Rapamycin has been reported to inhibit insulin-stimulated uptake of glucose by human adipocytes (Fig. 7*F*) (29). The insulin-stimulated phosphorylation of PKB at Ser-473 was, however, not affected by rapamycin (Fig. 7*G*). As expected, the diabetic state of the model is largely reproduced by the simulated effect of rapamycin inhibition of mTORC1, except for (i) the reduced internalization of IR, which in the diabetic state of the model is due to the reduced concentration of IR (supplemental Fig. S2); (ii) the dose-response curve for phosphorylation of PKB at Thr-308, which in the diabetic state of the model is a combined effect of reduced mTORC1 feedback to IRS1 and reduced concentration of IR (supplemental Fig. S2); and (iii) the basal and maximal stimulation of glucose uptake by insulin, which in the diabetic state of the model are the results of the reduced feedback from mTORC1 and reduced concentration of GLUT4 (supplemental Fig. S2). The importance of the feedback from mTORC1 to IRS1 also neatly explains enigmatic findings from phosphoproteomic screens in human embryonic kidney (HEK)-293E cells and mouse embryonic fibroblasts, which have demonstrated that most phosphorylation events stimulated by insulin are blocked by mTOR inhibition (30, 31).

Identification of Potential Drug Targets—Our model of insulin signaling in adipocytes, normally and in T2D, is driven by data exclusively from isolated human mature adipocytes. Therefore the model is directly relevant to human disease and has the potential for *in silico* identification of targets for treatment. We have demonstrated how the feedback from mTORC1 to IRS1 is attenuated in T2D and how this can cause the impairment observed in insulin signaling and much of the insulin-dependent uptake of glucose by the adipocytes (including a secondary reduction of GLUT4 levels through reduced mTORC1 activation of sterol regulatory element-binding protein 1). An obvious target for treatment is thus inhibition of the protein phosphatase that dephosphorylates IRS1 at Ser-307P. Simulating the diabetic state of the insulin-signaling model with such perturbation predicts that insulin sensitivity is fully restored (Fig. 8*A*), and that basal and maximal glucose uptake (which depends on the concentration of GLUT4) are only slightly

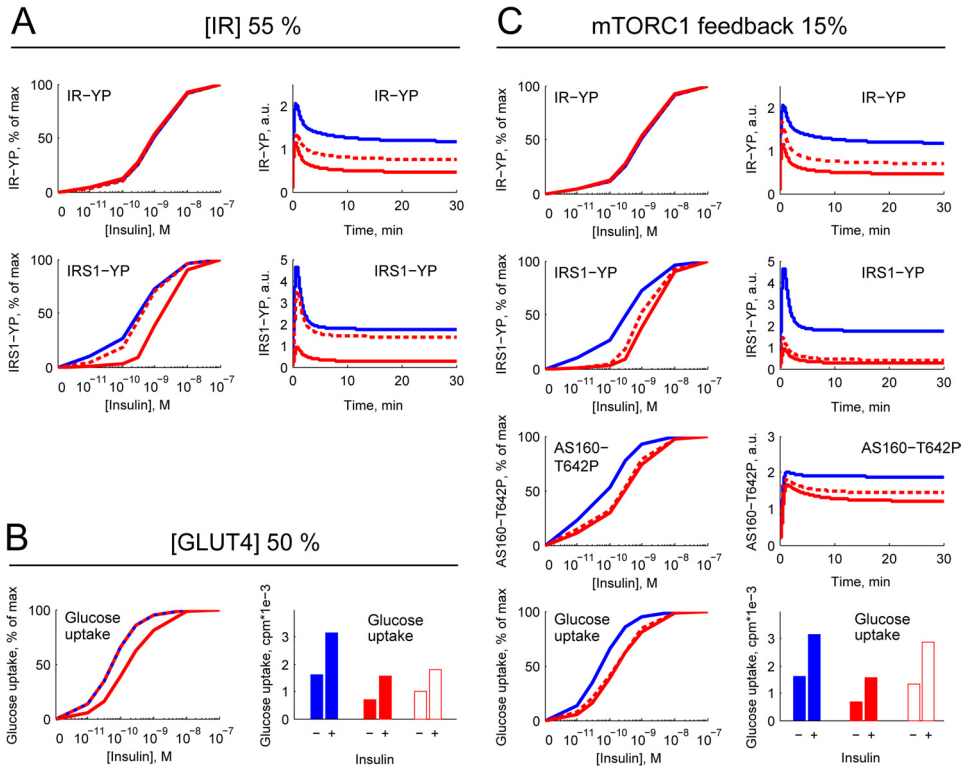

FIGURE 6. **Model analysis of the individual contribution of the three diabetes parameters to insulin resistance.** The simulated effect of reducing the concentration of IR (*A*) or GLUT4 (*B*), or reducing the feedback from mTORC1 to IRS1 (*C*) in the non-diabetic state of the detailed dynamic model (*red dotted lines*, *red open bars*) is compared with simulation of normal state (*blue lines*, *blue filled bars*) and simulation of diabetic state (*red lines*, *red filled bars*). A comprehensive analysis is shown in supplemental Fig. S2.

TABLE 2

Summary of experimentally measured variables and corresponding states in the model

Measured variable	Sum of states in model
IR-YP	*IRm-YP* + *IRi-YP*
Internalized IR	*IRi* + *IRi-YP*
IRS1-YP	*IRS1-YP* + *IRS1-YP-S307P*
IRS1-S307P	*IRS1-S307P* + *IRS1-YP-S307P*
PKB-T308P	*PKB-T308P* + *PKB-T308P-S473P*
PKB-S473P	*PKB-S473P* + *PKB-T308P-S473P*
AS160-T642P	*AS160-T642P*
S6K-T389P	*S6K-T389P*
S6-S235P/S236P	*S6-S235/236P*
Glucose uptake	*Glucose*
Active mTORC1	*mTORC1a*
Active mTORC2	*mTORC2a*

affected (Fig. 8*B*). This finds some experimental support when the dose-response phosphorylation of IRS1 at tyrosine in diabetic adipocytes was restored to normal after treating the cells with the phospho-serine/threonine protein phosphatase inhibitor okadaic acid, which also enhanced the phosphorylation of IRS1 at Ser-307 (10). Although okadaic acid will affect the state of phosphorylation of many cellular proteins, such as PKB, tyrosine phosphorylation of IRS1 is directly downstream of IR and is not directly affected by okadaic acid-inhibited serine/threonine protein phosphatases.

We have previously integrated a model of insulin signaling as an adipocyte submodel in a whole body model of glucose homeostasis of non-diabetic subjects (32). Using this multilevel model (33) we can evaluate potential drug targets in the context of glucose homeostasis during a meal. To simulate our detailed insulin-signaling model in this whole body context we first inserted our detailed insulin-signaling model in the multilevel model. We found that this comprehensive multilevel model explains glucose uptake by the adipose tissue during a meal (Fig. 8*C*, *blue*). Next, we used the diabetic version of the whole body model, with data obtained during intake of a meal by diabetic subjects (32), and adjusted the detailed insulin-signaling submodel to its diabetic state with the three diabetes parameters. This diabetic multilevel model can account also for glucose uptake by adipose tissue during a meal ingested by T2D patients (Fig. 8*C*, *red*). Using this multilevel model of glucose homeostasis in diabetes, we examined how an increase of the feedback from mTORC1 to IRS1 affects glucose uptake by adipose tissue in the diabetic whole body context. The resulting prediction of the multilevel model was an increase in the insulin-stimulated glucose uptake by the adipose tissue (Fig. 8*D*). Note that we restore insulin signaling only in the adipose tissue module and not in the other organ modules, for example, the insulin releasing module. Therefore, the multilevel model cannot fully restore normal dynamics of the adipose tissue glucose uptake. These results, nonetheless, demonstrate the potential of the developed multilevel insulin-signaling model.

DISCUSSION

The data presented herein are unique in the ways they have been obtained to construct a mathematical model of insulin signaling in type 2 diabetes of obesity. First, all data are obtained from human mature adipocytes, which is where the obesity related insulin resistance likely starts. This also means that all

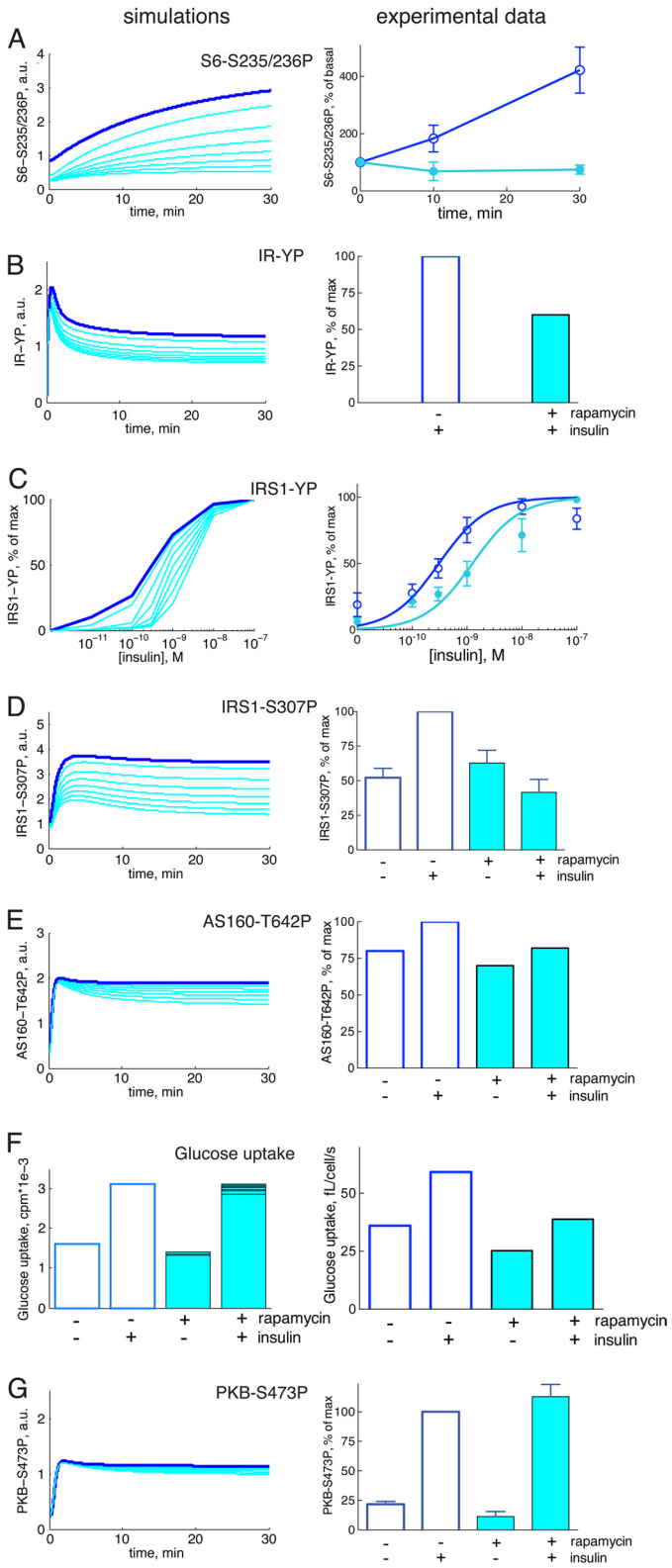

FIGURE 7. **Model analysis and experimental validation with inhibition of mTORC1.** Model simulations of the effect of rapamycin inhibition of mTORC1 (*cyan*) before stimulation with insulin (*left panels*) and experimental validation (*right panels*). The different lines in the model simulations represent the effect of 50, 75, 83, 88, 90, 92, and 93% inhibition of mTORC1. Simulations of the normal state (*blue*) are the same as in Fig. 5. A comprehensive model analysis with inhibition of mTORC1 is shown in supplemental Fig. S3. *A*, *left panel*, model simulation for phosphorylation of S6 at Ser-235/236 with (*cyan*) or without (*blue*) rapamycin inhibition of mTORC1. *Right panel*, adipocytes from non-diabetic subjects were preincubated with (*cyan*) ($n = 3$) or without (*blue*) ($n = 6$) 50 nM rapamycin for 30 min and then stimulated with 10 nM insulin for the indicated time, when cells were analyzed for the extent of phosphorylation of S6 at Ser-235/236 by SDS-PAGE and immunoblotting (mean ± S.E.) *B*, *left panel*, model simulation for phosphorylation of IR at tyrosine with (*cyan*) or without (*blue*) rapamycin inhibition of mTORC1. *Right panel*, adipocytes from non-diabetic subjects were preincubated with (*cyan*) or without (*blue*) 10 nM rapamycin for 15 min and then with 1000 microunits/ml of insulin for 15 min, when phosphorylation of IR at Tyr-1146 was analyzed by SDS-PAGE and immunoblotting. Data are from Ref. 29. *C*, *left panel*, model simulation for phosphorylation of IRS1 at tyrosine with (*cyan*) or without (*blue*) rapamycin inhibition of mTORC1. *Right panel*, adipocytes from non-diabetic subjects ($n = 5$) were preincubated with (*cyan*) or without (*blue*) 50 nM rapamycin for 30 min and then with the indicated concentration of insulin for 10 min, when phosphorylation of IRS1 at tyrosine was analyzed by SDS-PAGE and immunoblotting (mean ± S.E.). Data are from Ref. 10. *D*, *left panel*, model simulation for phosphorylation of IRS1 at Ser-307 with (*cyan*) or without (*blue*) rapamycin inhibition of mTORC1. *Right panel*, adipocytes from non-diabetic subjects ($n = 5$) were preincubated with (*cyan*) or without (*blue*) 50 nM rapamycin for 30 min and then with 100 nM insulin for 10 min, when phosphorylation of IRS1 at Ser-307 was analyzed by SDS-PAGE and immunoblotting (mean ± S.E.). Data are from Ref. 10. *E*, *left panel*, model simulation for phosphorylation of AS160 at Thr-642 with (*cyan*) or without (*blue*) rapamycin inhibition of mTORC1. *Right panel*, adipocytes from non-diabetic subjects were preincubated with (*cyan*) or without (*blue*) 10 nM rapamycin for 15 min and then with 1000 microunits/ml of insulin for 15 min, when phosphorylation of AS160 at Thr-642 was analyzed by SDS-PAGE and immunoblotting. Data are from Ref. 29. *F*, *left panel*, model simulation for insulin stimulation of glucose uptake with rapamycin inhibition of mTORC1. *Right panel*, human subcutaneous adipocytes from non-diabetic subjects ($n = 23$) were preincubated with 10 nM rapamycin for 15 min and then with 1000 microunits/ml of insulin for 15 min, when [^{14}C]glucose uptake was determined for 45 min. Data are from Ref. 29. *G*, *left panel*, model simulation for phosphorylation of PKB at Ser-473 with (*cyan*) or without (*blue*) rapamycin inhibition of mTORC1. *Right panel*, adipocytes from non-diabetic subjects were preincubated with (*cyan*) ($n = 3$) or without (*blue*) ($n = 8$) 50 nM rapamycin for 30 min and then stimulated with 10 nM insulin for 10 min, when cells were analyzed for the extent of phosphorylation of PKB at Ser-473 by SDS-PAGE and immunoblotting (mean ± S.E.).

data are from the same cell type. Second, data are collected throughout the signaling network, in a consistent fashion, allowing for combining the data in a systems analysis. Third, data are obtained in parallel with cells from both non-diabetic subjects and obese patients with T2D, making it possible to identify diabetes-specific signaling in T2D (which is a human disease). Fourth, the data consist of both dose-response data at quasi steady-states and relatively highly resolved time courses. Such time courses provide a crucial function in unraveling complex systems, especially using mathematical modeling. These data (supplemental Material) are thus also a valuable resource for future models incorporating data on additional signaling intermediaries and additional signaling branches of the network, *e.g.* to control of lipolysis.

To identify a systems wide mechanistic hypothesis is a complex task and we therefore took different and complementing approaches. First, we used traditional visual inspection and direct analysis of data, to identify how key signaling properties, such as time scales, sensitivity to insulin, and maximal effects of insulin, evolve through the network. Second, using conclusive minimal modeling (without relying on details in data and specific parameter values in the model) we rejected several hypotheses and showed that a feedback to IRS1 can explain the data. Third, through a dynamic mathematical model that takes all the details in data into account, we further refined understanding of the feedback to IRS1. This detailed dynamic model shows that although differences between normal and diabetic signaling appear throughout the system, the majority of them can be

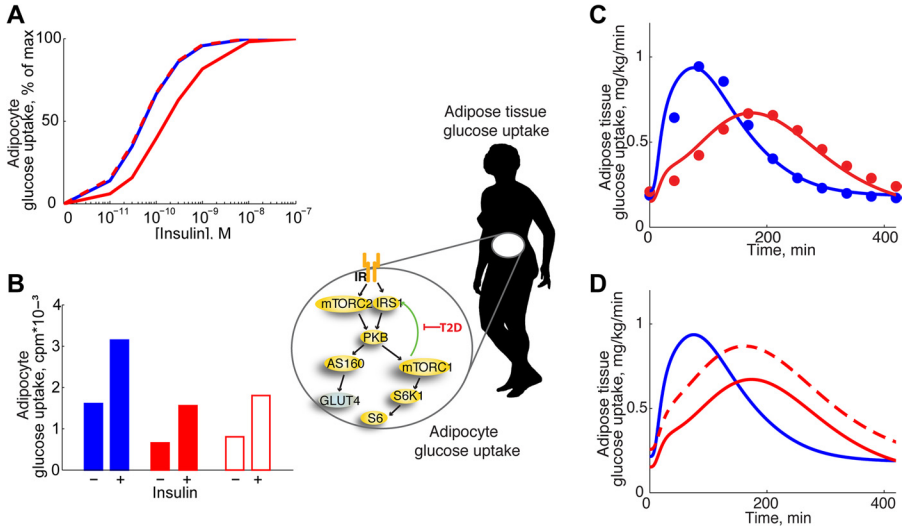

FIGURE 8. **Effects on glucose uptake at the cellular and whole body levels when treating T2D by increasing the feedback from mTORC1 to IRS1.** *A* and *B*, model simulations with the detailed mechanistic model of insulin signaling for the diabetic state, with a lowered rate of dephosphorylation of IRS1 at Ser-307 (*v2d* in Fig. 1*B*). *A,* glucose uptake by adipocytes in response to the indicated concentrations of insulin (*red dashed lines*) shows normalized insulin sensitivity. *B,* basal and maximal insulin-stimulated uptake of glucose (*red open bars*) are only slightly affected by the perturbation. *Continuous blue/red lines* and *filled blue/red bars* indicate model simulations of normal/diabetic adipocytes. *C* and *D,* model simulations, with the comprehensive combined whole body model, of glucose uptake by the adipose tissue in response to a meal. *C,* model simulations for normal subjects (*blue line*) compared with diabetic subjects (*red line*). Also indicated are calculated data from the whole body level models for normal non-diabetic (*blue dots*) and diabetic subjects (*red dots*). *D,* model simulations for diabetic subjects with a 10 times increased feedback from mTORC1 to IRS1 (red *dashed line*) compared with normal (*blue line*) and diabetic (*red line*) subjects.

explained by attenuation of a positive feedback from mTORC1 to IRS1 alone. The model we have developed is important because it constitutes a first quantitative systems wide description of the mechanisms involved in insulin signaling and insulin resistance in human adipocytes, which also includes a link to the whole body level. Moreover, key properties of the model were corroborated by independent experiments and we have demonstrated how the model can be used to simulate the action of drugs.

The model is relatively complex with many estimated parameters; it is therefore necessary to consider the robustness and uniqueness of the obtained conclusions. One aspect of robustness considers the choice of parameter values. In the model more than 40 parameters were fitted to data and the exact parameter values obtained are not unique. In particular, changes in the relative weight allotted to different aspects of data can affect model predictions. However, the qualitative minimal modeling was done in a conclusive fashion, such that those conclusions are not dependent on parameter values or weights in the cost function. Another type of robustness concerns the model structure. Our presented model is not the final description of insulin signaling and insulin resistance, but it is the first such model. Future work will provide improvements of the model structure, both regarding feedbacks and cross-talk with other signaling branches, such as insulin signaling through the MAP kinase pathway to mTORC1 and signaling for transcriptional control, as well as signaling in other cell types. In particular data on the antilipolytic action of insulin can extend our model to include control of lipolysis, which is a major metabolic function of the adipocytes and also a major aberration in T2D. Such an extension is consequently also important for the model to be really useful. This will be particularly interesting as it involves cross-talk with signaling through the β-adrenergic receptor and thus requires modeling the action of two interacting hormones.

The literature is replete with data implicating the phosphorylation of IRS1 at different serine/threonine residues in positive or negative control of insulin signaling and in positive or negative feedback loops of insulin signaling (16). The importance of cell type and experimental conditions implicating negative or positive effects is illustrated by the phosphorylation of IRS1 at serine 312 (human sequence, corresponding to serine 307 in murine sequence), an established negative effect in different experimental setups (34–36) that in a knock-in experiment eventually was found to have a positive effect on insulin signaling in mice *in vivo* (37). Examining different aspects of insulin signaling we (10–13) and others (14, 15) have previously found that phosphorylation of IRS1 at serine 307 in response to insulin is associated with a positive feedback. The systems approach we used herein demonstrates that a positive feedback to IRS1 can best explain the experimental data for the whole system. Although the phosphorylation of IRS1 at serine 307 fits the bill, parallel phosphorylation at other sites in IRS1 may convey or add to the positive feedback signal. Conclusive demonstration of the sites involved requires identification of all possible phosphorylation sites and their systematic evaluation. Nevertheless, our findings establish that a positive feedback signal to IRS1 is attenuated in T2D, and this was mimicked by different treatments that also inhibit phosphorylation of IRS1 at Ser-307: inhibition of mTORC1 with rapamycin (10), induction of insulin resistance with the adipokine RBP4 (11), and inhibition of mitochondrial function (13).

We found that activation of mTORC1 is attenuated in adipocytes from patients with T2D whether or not they were on treatment with the insulin-sensitizing drug metformin (Fig. 9). In addition, attenuation of mTORC1 activity in adipocytes

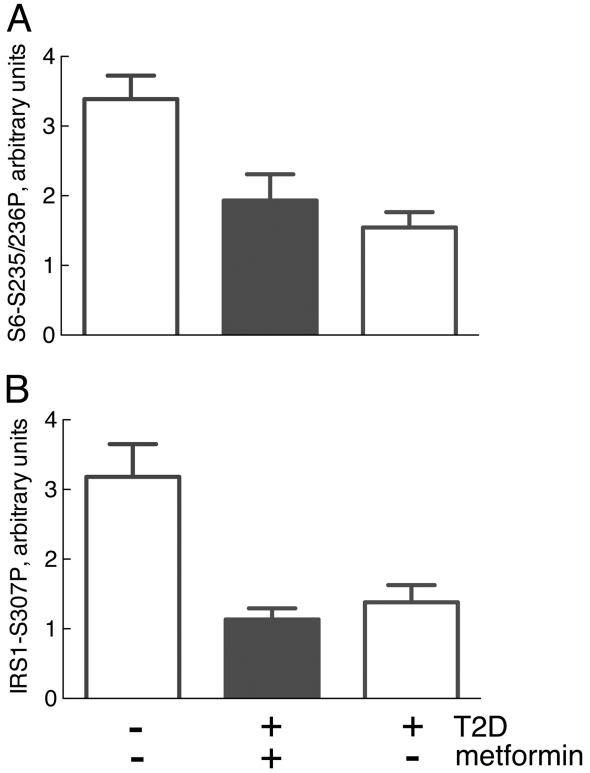

FIGURE 9. **Attenuated mTORC1 signaling in adipocytes from T2D patients with or without metformin treatment.** Adipocytes were obtained from non-diabetic or T2D subjects (as indicated). Patients with T2D had not received any medication for T2D or had received metformin (as indicated) as part of their treatment prior to surgery and tissue biopsy. The adipocytes were incubated with insulin at 10 nM until steady-state phosphorylation (40 min for S6 and 10 min for IRS1), when cells were analyzed by SDS-PAGE and immunoblotting for the extent of phosphorylation of S6 at Ser-235/236 (*A*) and phosphorylation of IRS1 at Ser-307 (*B*). Results are presented as mean ± S.E. for triplicate cell determinations of 7 subjects (non-diabetic), 3 subjects (T2D with metformin treatment prior to surgery), and 3 subjects (T2D without metformin treatment).

from non-diabetic subjects also directly correlates with the extent of insulin resistance of the adipocyte donors (13). This is important as many conditions associated with insulin resistance, such as inflammation, ER-stress, hypoxia, and mitochondrial dysfunction, are all well known to inhibit mTORC1. Unfortunately it is not possible to draw any strong conclusions from the knock-out of mTORC1 regarding its normal function in human adipocytes. In animal studies, adipose specific knock-out of raptor has caused partial transdifferentiation of white adipocytes to brown, with *e.g.* expression of the mitochondrial uncoupling protein UCP1 (38). Also, whereas knock-out of either raptor (39) or rictor (40) in muscle has generated mice with impaired glucose tolerance, knock-out of mTOR (41) does not affect glucose tolerance.

It should be noted that our data and model describe the two states, non-diabetes and diabetes, and are not describing the transition from the non-diabetic to the diabetic state, although they do suggest possible pathogenic mechanisms of insulin resistance. Attenuation of mTORC1 activity may be a logical response to obesity considering that, although the size of human adipocytes vary, their maximal size appears to be <0.3 mm in diameter (42). Cells can only get so big, there is an upper limit beyond which cellular integrity and function are compromised. Attenuation of mTORC1 signaling is an effective means for the adipocyte to restrict accumulation of triacylglycerol and further cell growth. Indeed it has been reported that large adipocytes are more insulin resistant than smaller from the same individual (43, 44), that there are more small adipocytes in obese insulin-sensitive compared with obese insulin-resistant individuals (42), that adipocyte size predicts incidence of T2D (45), and that the inhibitory effect of rapamycin on insulin stimulation of glucose transport is related to the size of the adipocytes (29). It can be noted that this mechanism for insulin resistance in obesity is in concord with the current view of how obesity induces insulin resistance in other tissues through ectopic storage of fat as a result of filled adipose stores (reviewed in Ref. 46). It remains to understand how mTORC1 can sense and respond to cell size. However, a disappointing implication is that insulin resistance in adipocytes cannot be cured by restoring insulin signaling; not without consequences such as necrosis of oversized cells. Instead, recruiting more adipocytes to relieve the pressure on big cells should improve insulin sensitivity. Interestingly, this is a mechanism of action of the thiazolidinedione class of peroxisome proliferator-activated receptor-γ agonists (47) that have been widely used to successfully improve insulin sensitivity in the adipose tissue in treatment of T2D.

Acknowledgments—We thank Dr. Preben Kjølhede for unfailingly supplying biopsies from surgery and Annelie Castell, Dr. Anna Danielsson, Niklas Hed, David Janzén, David Jullesson, and Dr. Anita Öst for their involvement in some of the experimental or modeling work.

REFERENCES

1. Nyman, E., Cedersund, G., and Strålfors, P. (2012) Insulin signaling. Mathematical modeling comes of age. *Trends Endocrinol. Metab.* **23,** 107–115
2. Kiselyov, V. V., Versteyhe, S., Gauguin, L., and De Meyts, P. (2009) Harmonic oscillator model of the insulin and IGF1 receptors' allosteric binding and activation. *Mol. Syst. Biol.* **5,** 243
3. Brännmark, C., Palmér, R., Glad, S. T., Cedersund, G., and Strålfors, P. (2010) Mass and information feedbacks through receptor endocytosis govern insulin signaling as revealed using a parameter-free modeling framework. *J. Biol. Chem.* **285,** 20171–20179
4. Dalle Pezze, P., Sonntag, A. G., Thien, A., Prentzell, M. T., Gödel, M., Fischer, S., Neumann-Haefelin, E., Huber, T. B., Baumeister, R., Shanley, D. P., and Thedieck, K. (2012) A dynamic network model of mTOR signaling reveals TSC-independent mTORC2 regulation. *Sci. Signal.* **5,** ra25
5. Danielsson, A., Ost, A., Lystedt, E., Kjolhede, P., Gustavsson, J., Nystrom, F. H., and Strålfors, P. (2005) Insulin resistance in human adipocytes downstream of IRS1 after surgical cell isolation, but at the level of phosphorylation of IRS1 in type 2 diabetes. *FEBS J.* **272,** 141–151
6. Strålfors, P., and Honnor, R. C. (1989) Insulin-induced dephosphorylation of hormone-sensitive lipase. Correlation with lipolysis and cAMP-dependent protein kinase activity. *Eur. J. Biochem.* **182,** 379–385
7. Frost, S. C., Kohanski, R. A., and Lane, M. D. (1987) Effect of phenylarsine oxide on insulin-dependent protein phosphorylation and glucose transport in 3T3-L1 adipocytes. *J. Biol. Chem.* **262,** 9872–9876
8. Schmidt, H., and Jirstrand, M. (2006) Systems Biology Toolbox for MATLAB. A computational platform for research in systems biology. *Bioinformatics* **22,** 514–515
9. Laplante, M., and Sabatini, D. M. (2012) mTOR signaling in growth control and disease. *Cell* **149,** 274–293

10. Danielsson, A., Ost, A., Nystrom, F. H., and Strålfors, P. (2005) Attenuation of insulin-stimulated insulin receptor substrate-1 serine 307 phosphorylation in insulin resistance of type 2 diabetes. *J. Biol. Chem.* **280,** 34389–34392
11. Ost, A., Danielsson, A., Lidén, M., Eriksson, U., Nystrom, F. H., and Strålfors, P. (2007) Retinol-binding protein-4 attenuates insulin-induced phosphorylation of IRS1 and ERK1/2 in primary human adipocytes. *FASEB J.* **21,** 3696–3704
12. Danielsson, A., Fagerholm, S., Ost, A., Franck, N., Kjolhede, P., Nystrom, F. H., and Strålfors, P. (2009) Short-term over-eating induces insulin resistance in fat cells in lean human subjects. *Mol. Med.* **15,** 228–234
13. Ost, A., Svensson, K., Ruishalme, I., Brännmark, C., Franck, N., Krook, H., Sandström, P., Kjolhede, P., and Strålfors, P. (2010) Attenuated mTOR signaling and enhanced autophagy in adipocytes from obese patients with type 2 diabetes. *Mol. Med.* **16,** 235–246
14. Giraud, J., Leshan, R., Lee, Y. H., and White, M. F. (2004) Nutrient-dependent and insulin-stimulated phosphorylation of insulin receptor substrate-1 on serine 302 correlates with increased insulin signaling. *J. Biol. Chem.* **279,** 3447–3454
15. Weigert, C., Kron, M., Kalbacher, H., Pohl, A. K., Runge, H., Häring, H. U., Schleicher, E., and Lehmann, R. (2008) Interplay and effects of temporal changes in the phosphorylation state of serine-302, -307, and -318 of insulin receptor substrate-1 on insulin action in skeletal muscle cells. *Mol. Endocrinol.* **22,** 2729–2740
16. Copps, K. D., and White, M. F. (2012) Regulation of insulin sensitivity by serine/threonine phosphorylation of insulin recceptor substrate proteins IRS1 and IRS2. *Diabetologia* **55,** 2565–2582
17. Cedersund, G. (2012) Conclusions via unique predictions obtained despite unidentifiability. New definitions and a general method. *FEBS J.* **279,** 3513–3527
18. Olefsky, J. M. (1976) Decreased insulin binding to adipocytes and circulating monocytes from obese subjects. *J. Clin. Invest.* **57,** 1165–1172
19. Werner, E. D., Lee, J., Hansen, L., Yuan, M., and Shoelson, S. E. (2004) Insulin resistance due to phosphorylation of insulin receptor substrate-1 at serine 302. *J. Biol. Chem.* **279,** 35298–35305
20. Harrington, L. S., Findlay, G. M., Gray, A., Tolkacheva, T., Wigfield, S., Rebholz, H., Barnett, J., Leslie, N. R., Cheng, S., Shepherd, P. R., Gout, I., Downes, C. P., and Lamb, R. F. (2004) The TSC1–2 tumor suppressor controls insulin–PI3K signaling via regulation of IRS proteins. *J. Cell Biol.* **166,** 213–223
21. Carvalho, E., Jansson, P. A., Axelsen, M., Eriksson, J. W., Huang, X., Groop, L., Rondinone, C., Sjöström, L., and Smith, U. (1999) Low cellular *IRS1* gene and protein expression predict insulin resistance and NIDDM. *FASEB J.* **13,** 2173–2178
22. Maianu, L., Keller, S. R., and Garvey, W. T. (2001) Adipocytes exhibit abnormal subcellular distribution and translocation of vesicles containing glucose transporter 4 and insulin-regulated aminopeptidase in type 2 diabetes mellitus. Implications regarding defects in vesicle trafficking. *J. Clin. Endocrinol. Metab.* **86,** 5450–5456
23. Hussey, S. E., McGee, S. L., Garnham, A., Wentworth, J. M., Jeukendrup, A. E., and Hargreaves, M. (2011) Exercise training increases adipose tissue GLUT4 expression in patients with type 2 diabetes. *Diabetes Obes. Metab.* **13,** 959–962
24. Kampmann, U., Christensen, B., Nielsen, T. S., Pedersen, S. B., Ørskov, L., Lund, S., Møller, N., and Jessen, N. (2011) GLUT4 and UBC9 protein expression is reduced in muscle from diabetic patients with severe insulin resistance. *PLoS ONE* **6,** e27854
25. Im, S. S., Kwon, S. K., Kang, S. Y., Kim, T. H., Kim, H. I., Hur, M. W., Kim, K. S., and Ahn, Y. H. (2006) Regulation of *GLUT4* gene expression by SREPB-1c in adipocytes. *Biochem. J.* **399,** 131–139
26. Porstmann, T., Santos, C. R., Griffiths, B., Cully, M., Wu, M., Leevers, S., Griffiths, J. R., Chung, Y. L., and Schulze, A. (2008) SREBP activity is regulated by mTORC1 and contributes to Akt-dependent cell growth. *Cell Metab.* **8,** 224–236
27. Peterson, T. R., Sengupta, S. S., Harris, T. E., Carmack, A. E., Kang, S. A., Balderas, E., Guertin, D. A., Madden, K. L., Carpenter, A. E., Finck, B. N., and Sabatini, D. M. (2011) mTOR complex 1 regulates Lipin 1 localization to control the SREBP pathway. *Cell* **146,** 408–420
28. Zhou, L., Zhang, J., Fang, Q., Liu, M., Liu, X., Jia, W., Dong, L. Q., and Liu, F. (2009) Autophagy-mediated insulin receptor down-regulation contributes to endoplasmic reticulum stress-induced insulin resistance. *Mol. Pharmacol.* **76,** 596–603
29. Pereira, M. J., Palming, J., Rizell, M., Aureliano, M., Carvalho, E., Svensson, M. K., and Eriksson, J. W. (2012) mTOR inhibition with rapamycin causes impaired insulin signalling and glucose uptake in human subcutaneous and omental adipocytes. *Mol. Cell. Endocrinol.* **355,** 96–105
30. Hsu, P. P., Kang, S. A., Rameseder, J., Zhang, Y., Ottina, K. A., Lim, D., Peterson, T. R., Choi, Y., Gray, N. S., Yaffe, M. B., Marto, J. A., and Sabatini, D. M. (2011) The mTOR-regulated phosphoproteome reveals a mechanism of mTORC-1mediated inhibition of growth factor signalling. *Science* **332,** 1317–1322
31. Yu, Y., Yoon, S. O., Poulogiannis, G., Yang, Q., Ma, X. M., Villén, J., Kubica, N., Hoffman, G. R., Cantley, L. C., Gygi, S. P., and Blenis, J. (2011) Phosphoproteomic analysis identifies Grb10 as an mTORC1 substrate that negatively regulates insulin signaling. *Science* **332,** 1322–1326
32. Dalla Man, C., Rizza, R. A., and Cobelli, C. (2007) Meal simulation model of the glucose-insulin system. *IEEE Trans. Biomed. Eng.* **54,** 1740–1749
33. Nyman, E., Brännmark, C., Palmér, R., Brugård, J., Nyström, F. H., Strålfors, P., and Cedersund, G. (2011) A hierarchical whole body modeling approach elucidates the link between *in vitro* insulin signaling and *in vivo* glucose homeostasis. *J. Biol. Chem.* **286,** 26028–26041
34. Um, S. H., D'Alessio, D., and Thomas, G. (2006) Nutrient overload, insulin resistance, and ribosomal protein S6 kinase 1, S6K1. *Cell Metab.* **3,** 393–402
35. Aguirre, V., Uchida, T., Yenush, L., Davis, R., and White, M. F. (2000) The c-*jun* NH_2-terminal kinase promotes insulin resistance during association with insulin receptor substrate-1 and phosphorylation of Ser-307. *J. Biol. Chem.* **275,** 9047–9054
36. Yu, C., Chen, Y., Cline, G. W., Zhang, D., Zong, H., Wang, Y., Bergeron, R., Kim, J. K., Cushman, S. W., Cooney, G. J., Atcheson, B., White, M. F., Kraegen, E. W., and Shulman, G. I. (2002) Mechanism by which fatty acids inhibit insulin activation of insulin receptor substrate-1 (IRS-1)-associated phosphatidylinositol 3-kinase activity in muscle. *J. Biol. Chem.* **277,** 50230–50236
37. Copps, K. D., Hancer, N. J., Opare-Ado, L., Qiu, W., Walsh, C., and White, M. F. (2010) Irs1 serine 307 promotes insulin sensitivity in mice. *Cell Metab.* **11,** 84–92
38. Polak, P., Cybulski, N., Feige, J. N., Auwerx, J., Rüegg, M. A., and Hall, M. N. (2008) Adipose-specific knockout of raptor results in lean mice with enhanced mitochondrial respiration. *Cell Metab.* **8,** 399–410
39. Bentzinger, C. F., Romanino, K., Cloëtta, D., Lin, S., Mascarenhas, J. B., Oliveri, F., Xia, J., Casanova, E., Costa, C. F., Brink, M., Zorzato, F., Hall, M. N., and Rüegg, M. A. (2008) Skeletal muscle-specific ablation of raptor, but not rictor, causes metabolic changes and results in muscle dystrophy. *Cell Metab.* **8,** 411–424
40. Kumar, A., Harris, T. E., Keller, S. R., Choi, K. M., Magnuson, M. A., and Lawrence, J. C. (2008) Muscle-specific deletion of rictor impairs insulin-stimulated glucose transport and enhances basal glycogen synthase activity. *Mol. Cell. Biol.* **28,** 61–70
41. Risson, V., Mazelin, L., Roceri, M., Sanchez, H., Moncollin, V., Corneloup, C., Richard-Bulteau, H., Vignaud, A., Baas, D., Defour, A., Freyssenet, D., Tanti, J. F., Le-Marchand-Brustel, Y., Ferrier, B., Conjard-Duplany, A., Romanino, K., Bauché, S., Hantaï, D., Mueller, M., Kozma, S. C., Thomas, G., Rüegg, M. A., Ferry, A., Pende, M., Bigard, X., Koulmann, N., Schaeffer, L., and Gangloff, Y. G. (2009) Muscle inactivation of mTOR causes metabolic and dystrophin defects leading to severe myopathy. *J. Cell Biol.* **187,** 859–874
42. Klöting, N., Fasshauer, M., Dietrich, A., Kovacs, P., Schön, M. R., Kern, M., Stumvoll, M., and Blüher, M. (2010) Insulin-sensitive obesity. *Am. J. Physiol. Endocrinol. Metab.* **299,** E506–515
43. Franck, N., Stenkula, K. G., Ost, A., Lindström, T., Strålfors, P., and Nystrom, F. H. (2007) Insulin-induced GLUT4 translocation to the plasma membrane is blunted in large compared with small fat cells isolated from the same subjects. *Diabetologia* **50,** 1716–1722
44. Laurencikiene, J., Skurk, T., Kulyté, A., Hedén, P., Aström, G., Sjölin, E., Rydén, M., Hauner, H., and Arner, P. (2011) Regulation of lipolysis in small

and large fat cells of the same subject. *J. Clin. Endocrinol. Metab.* **96,** E2045-E2049
45. Lönn, M., Mehlig, K., Bengtsson, C., and Lissner, L. (2010) Adipocyte size predicts incidence of type 2 diabetes in women. *FASEB J.* **24,** 326–331
46. Samuel, V. T., and Shulman, G. I. (2012) Mechanisms for insulin resistance. Common threads and missing links. *Cell* **148,** 852–871
47. de Souza, C. J., Eckhardt, M., Gagen, K., Dong, M., Chen, W., Laurent, D., and Burkey, B. F. (2001) Effects of pioglitazone on adipose tissue remodeling within the setting of obesity ad insulin resistance. *Diabetes* **50,** 1863–1871
48. Raue, A., Kreutz, C., Maiwald, T., Bachmann, J., Schilling, M., Klingmüller, U., and Timmer, J. (2009) Structural and practical identifiability analysis of partially observed dynamical models by exploiting the profile likelihood. *Bioinformatics* **25,** 1923–1929